Inorg. Chem. **1993,** *32,* 977–987

Oxidation of Nickel Thiolate Ligands by Dioxygen

Shaukat A. Mirza, Michelle A. Pressler, Manoj Kumar, Roberta O. Day, and Michael J. Maroney*

Department of Chemistry, University of Massachusetts, Amherst, Massachusetts 01003

Received August 20, 1992

The reactions of Ni complexes of the tridentate dithiolate ligands $RN(CH_2CH_2S^-)_2$ and $S(CH_2CH_2S^-)_2$ with O_2 leading to the formation of complexes containing one S-bound sulfinate ligand are described. Reaction of the ligands with $Ni(OAc)_2$ yields dinuclear $[Ni(L)]_2$ complexes. Reaction of these dimers with $Et_4N(CN)$ yields Et_4N^+ salts of the four-coordinate complex anions, $[Ni(L)CN]^-$. For two of the ligands in the series presented, *N,N*-bis(2-mercaptoethyl)-2-(methylthio)ethylamine (**2**) and bis(2-mercaptoethyl) sulfide (**6**), crystals of the compounds have been obtained and structurally characterized by single crystal X-ray diffraction. $Et_4N[Ni(\mathbf{2})CN]$ crystallizes in monoclinic space group $P2_1/c$ with cell dimensions $a = 12.803(8)$ Å, $b = 12.713(9)$ Å, $c = 14.788(12)$ Å, $\beta = 119.31(6)°$, $V = 2098.8$ Å^3, and $Z = 4$. The structure was refined to $R = 0.087$ and $R_w = 0.106$. The anion consists of an essentially planar Ni(II) complex with two trans-oriented thiolate ligands, one tertiary amine N-donor atom, and one cyanide ligand. $Et_4N[Ni(\mathbf{6})CN]$ crystallizes in orthorhombic space group $P2_12_12_1$ with cell dimensions $a = 8.871(2)$ Å, $b = 11.505(2)$ Å, $c = 17.767(2)$ Å, $V = 1813.3$ Å^3, and $Z = 4$. The structure was refined to $R = 0.044$ and $R_w = 0.064$. The anion consists of a highly distorted planar Ni(II) complex with two trans-oriented thiolate ligands, one thioether S-donor atom, and one cyanide ligand, where the thioether S-donor atom lies significantly out of the plane described by Ni and the remaining donor atoms. The anion exhibits two conformations in the crystal involving placement of the thioether S-donor atom above or below this plane. The $[Ni(L)CN]^-$ anions are air sensitive and react with O_2 to form planar Ni(II) complex anions with one thiolate and one sulfinate ligand, $[Ni(L\text{-}O_2)CN]^-$. $Et_4N[Ni(\mathbf{2}\text{-}\mathbf{O_2})CN]$ crystallizes in monoclinic space group $P2_1/c$ with cell dimensions $a = 12.784(4)$ Å, $b = 12.757(2)$ Å, $c = 14.847(4)$ Å, $\beta = 115.00(3)°$, $V = 2194.5$ Å^3, and $Z = 4$. The structure was refined to $R = 0.033$ and $R_w = 0.042$. Oxygen uptake measurements reveal that the oxidation processes have a stoichiometry of 1:1 O_2:Ni. The oxidations were followed spectrophotometrically. Kinetic analysis of the data reveals that the reactions obey the following rate law: $d[[Ni(L\text{-}O_2)CN]^-]/dt = k[[Ni(L)CN]^-][O_2]$. Measurements of the rate of oxidation at 30 °C under constant $[O_2] = 1$ atm yield pseudo-first-order rate constants, $k_{obs} = (0.72(2)–1.60(1)) \times 10^{-4}$ s^{-1} for the amine ligands. Second-order rate constants were determined to be $(1.4–3.1) \times 10^{-2}$ M^{-1} s^{-1} at 30 °C in DMF. The reaction of $[Ni(\mathbf{6})CN]^-$ is 2–5 times slower than those of the tertiary amine ligands. The dependence of the reactions on the ligand donor atom sets, the N-substituents, the solvent, and the addition of radical and $^1O_2$ scavengers is discussed. Reactions conducted with isotopically labeled O_2 gas mixtures reveal that the sulfinate oxygen atoms in the products derive principally from a single O_2 molecule. A mechanism involving the formation of thiadioxirane intermediates is proposed, with the rate-determining step being the cleavage of the O–O bond. The possible relevance of the chemistry involved to the biological oxidation of cysteine by metalloenzymes is also discussed.

The redox chemistry of thiols plays key roles in many biological processes.[1-3] The important biochemical oxidations of cysteine include its conversion to disulfides (cystine) and the formation of oxy acids such as cysteine sulfenic acid, cysteine sulfinic acid (CSA) and hypotaurine (2-aminoethanesulfinic acid), cysteic acid (cysteine sulfonic acid), and taurine (2-aminoethanesulfonic acid). The oxidation of cysteine residues in proteins and the role of metal ions in catalyzing these oxidations have been reviewed.[4-6] In several cases, evidence supporting the oxidation of active site cysteine sulfhydryl groups in the deactivation of enzymes has accumulated. In the case of oxidation to cysteine sulfenic acid, the oxidation is readily reversed to reactivate the enzymes. Our interest in the reversible deactivation of Ni containing hydrogenases (H_2ases) by O_2 provided the impetus to investigate the oxidation of Ni thiolate complexes by molecular oxygen. These studies led to the discovery that Ni thiolates can be converted to S-bonded sulfinato complexes by incorporation of dioxygen (a four electron oxidation process), and provided the first structurally characterized example of a sulfinato complex derived from the oxidation of a transition metal thiolate complex by O_2.[7] Here we report studies of a series of Ni thiolate complexes that provide insights into the novel reaction mechanism of this oxidation and carry implications for biological cysteine oxidation.

Results

Synthesis and Characterization. The tridentate ligands $RN(CH_2CH_2SH)_2$ (R = CH_3 (**1**),[8] $CH_2CH_2SCH_3$ (**2**)[9]) were synthesized by literature procedures, except that the methyl derivative was isolated as a monohydrochloride salt. Attempts to isolate this ligand by vacuum distillation led to large amounts of decomposition products. The remaining bis(2-mercaptoethyl)amine ligands (R = $CH_2CH_2SCH_2Ph$ (**3**), $CH_2CH_2CH(Ph)_2$ (**4**), and CH_2Ph (**5**)) were synthesized from the primary amines by reaction with ethylene sulfide, in analogy with the procedure given for **2**, and isolated as monohydrochloride salts. The tridentate ligand bis(2-mercaptoethyl)sulfide, $S(CH_2CH_2SH)_2$

---

[1] *Sulfur-Centered Reactive Intermediates in Chemistry and Biology*; Chatgilialoglu, C., Asmus, K-D., Eds.; Plenum Press: New York, 1990.

[2] Huxtable, R. J. *Biochemistry of Sulfur*; Plenum Press: New York, 1986.

[3] Fluharty, A. L. *The Chemistry of the Thiol Group*; Patai, S., Ed.; John Wiley and Sons: New York, 1974; Chapter 13.

[4] Friedman, M. *Chemistry and Biochemistry of the Sulfhydryl Group in Amino Acids, Peptides, and Proteins*; Pergamon Press: New York, 1973.

[5] Jocelyn, P. C. *Biochemistry of the SH Group*; Academic Press: New York, 1972.

[6] Allison, W. S. *Acc. Chem. Res.* **1976**, *9*, 293.

[7] Kumar, M.; Colpas, G. J.; Day, R. O.; Maroney, M. J. *J. Am. Chem. Soc.* **1989**, *111*, 8323.

[8] Harley-Mason, J. *J. Chem. Soc.* **1947**, 320.

[9] Corbin, J. L.; Miller, K. F.; Pariyadath, N.; Wherland, S.; Bruce, A. E.; Stiefel, E. I. *Inorg. Chim. Acta* **1984**, *90*, 41.

0020-1669/93/1332-0977$04.00/0

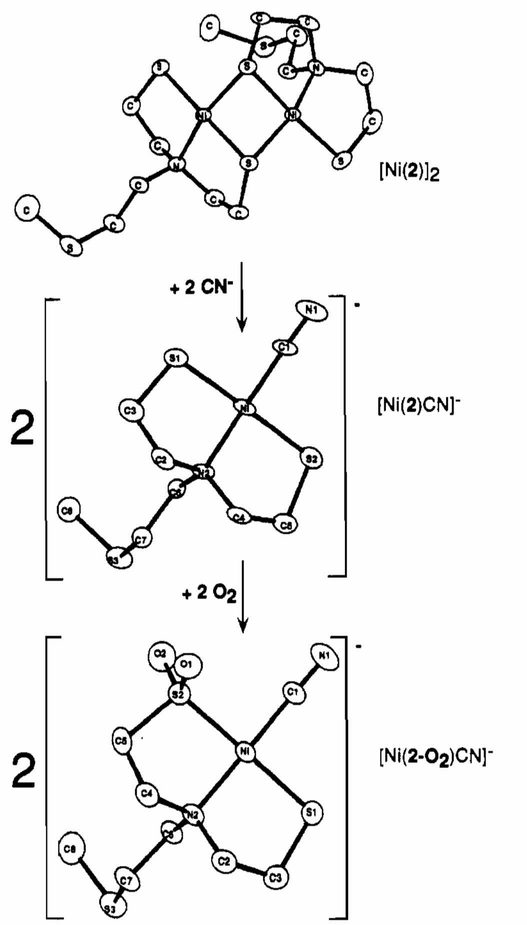

Figure 1. The reaction of $[Ni(\mathbf{2})]_2$ with CN^- and subsequent oxidation of $[Ni(\mathbf{2})CN]^-$ by O_2. The molecules are shown as ORTEP plots with thermal ellipsoids at the 30% probability level.

(**6**), was obtained commercially. Synthetic details and IR spectral data for the ligands and their metal complexes are compiled in the Experimental Section.

Reaction of the tridentate ligands (L) with $Ni(OAc)_2$ yields the dark red-brown, air stable, dinuclear Ni complexes, $[Ni(L)]_2$, as previously reported for L = **2**,[10] **6**.[11] In the syntheses employing hydrochloride salts, one equivalent of triethylamine was added. The structure of a representative $[Ni(L)]_2$ complex, $[Ni(\mathbf{2})]_2$, is shown in Figure 1, which also describes a typical oxidation reaction. The structure of $[Ni(\mathbf{2})]_2$ has been previously reported,[10] and consists of edge-sharing approximately planar $Ni(NS_3)$ units. The Ni donor atoms consist of a tertiary amine N atom, one terminal thiolate, and two bridging thiolate ligands, one of which is derived from the ligand bound to the second Ni center in the dinuclear complex. The electronic absorption spectra of the $[Ni(L)]_2$ complexes (Table I) exhibit characteristic features at ca. 290, 310, 340, 380, 440, and 550 nm with absorbances in the UV region that are less intense than the CN^- containing products. The thioether containing dimer, $[Ni(\mathbf{6})]_2$, has a similar spectrum with absorptions at 277, 308, 387, and 511 nm, all of which must be due to S → Ni LMCT, since the ligand does not absorb above 270 nm. Bands in the 240–340 nm region of various thiolato complexes have been assigned to $RS^- \rightarrow M$ LMCT transitions.[12-14] The presence of shoulders at 340 and 440 nm in the spectra of complexes of the amine ligands that are absent in the spectra of the complex of the thioether ligand suggests that these bands are associated with charge transfer from the N donor atom.

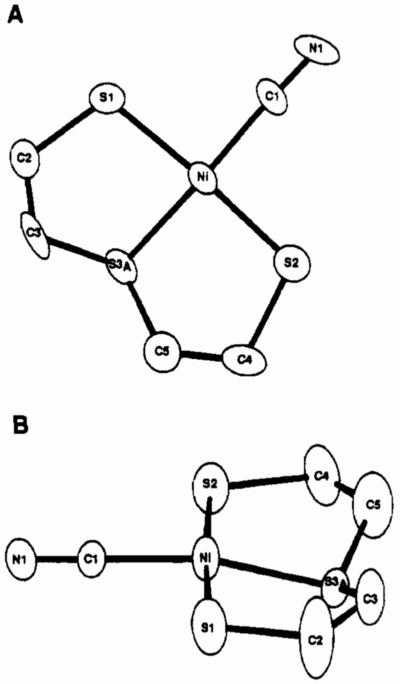

Figure 2. ORTEP plots of $Et_4N[Ni(\mathbf{6})CN]^-$ (A) with thermal ellipsoids at the 30% probability level. The cation and hydrogen atoms have been omitted for clarity. A: Top view illustrating connectivity. B: Side view emphasizing non-planarity of thioether S-donor atom.

The cyanide complexes, $Et_4N[Ni(L)CN]$, were obtained by reacting $[Ni(L)]_2$ with $Et_4N(CN)$, where the CN^- ligand replaces bridging thiolate ligands and forms planar trans-dithiolato complexes. These dark green diamagnetic complexes are deliquescent solids, air sensitive in solution, and were generally not isolated but were prepared and used in solution. The electronic absorption spectra of these complexes (Table I) have characteristic absorptions near 275, 310, and 420 nm. The spectrum obtained for the complex with the thioether ligand, $[Ni(\mathbf{6})CN]^-$, is similar to the spectra obtained from complexes containing amine ligands. IR spectra obtained on the complexes reveal bands characteristic of the ligands, including ν_{CN} near 2100 cm^{-1} for the CN^- ligand (see Experimental Section).

The complexes $Et_4N[Ni(\mathbf{2})CN]$ and $Et_4N[Ni(\mathbf{6})CN]$ were isolated and crystallized for single crystal X-ray diffraction experiments. Crystallographic data for these compounds are reported in Table II. The structures of the $[Ni(\mathbf{2})CN]^-$ and $[Ni(\mathbf{6})CN]^-$ anions are shown in Figures 1 and 2, respectively. Selected atomic coordinates, bond lengths and angles for the anions are reported in Tables III, IV, and VI.

The geometry at the Ni center in $[Ni(\mathbf{2})CN]^-$ is essentially planar, with the Ni and ligand donor atoms (S1, S2, C1, N2) coplanar to within ±0.045(7) Å. This is in contrast to the structure of the $[Ni(\mathbf{6})CN]^-$, where two clearly discernible positions were found for the thioether S-donor atom. The details of this structure are somewhat compromised by the disorder present; the remaining atomic positions represent the average values to the extent that the positions in question are sensitive to the position of the thioether S-donor atom. Despite these limitations, it does appear that the geometry at the Ni is distorted from a planar structure, where the two positions for the thioether S-donor atom lie above and below the plane defined by the Ni and the remaining three ligand donor atoms (S1, S2, and C1). The two positions occupied by the thioether S atom (S3) are displaced in opposite directions from this plane by distances of 0.562(4) Å (S3A) and 0.685(6) Å (S3B). The bond lengths in the two anions are unremarkable. The $Ni–S_{thiolate}$ distances for both compounds fall in the established

---

(10) Colpas, G. J.; Kumar, M.; Day, R. O.; Maroney, M. J. *Inorg. Chem.* **1990**, *29*, 4779.

(11) (a) Harley-Mason, J. *J. Chem. Soc.* **1952**, 146. (b) Barclay, G. A.; McPartlin, E. M.; Stephenson, N. C. *Acta Crystallogr.* **1969**, *b25*, 1262. (c) Baker, D. J.; Goodall, D. C.; Moss, D. S. *Chem. Commun.* **1969**, 325.

(12) Weschler, C. J.; Deutsch, E. *Inorg. Chem.* **1976**, *15*, 139.

(13) Adzamli, I. K.; Deutsch, E. *Inorg. Chem.* **1980**, *19*, 1366.

(14) Weschler, C. J.; Deutsch, E. *Inorg. Chem.* **1973**, *12*, 2682.

Table I. Electronic Absorption Spectral Data

complex	solvent	λ_{max}, nm (ϵ,[a] $M^{-1}\ cm^{-1}$)	isosbestic pts,[b] nm
[Ni(**1**)]$_2$	DMF	289 (6280); 312 (5970); 340 (sh); 376 (sh); 432 (sh); 552 (570)	
	CH_3CN	286 (7400); 310 (6890); 338 (sh); 376 (sh); 435 (sh); 551 (615)	
[Ni(**2**)]$_2$	DMF	292 (7410); 308 (sh); 341 (sh); 383 (sh); 440 (1050); 547 (750)	
	CH_3CN	291 (6080); 308 (sh); 340 (sh); 380 (sh); 443 (sh); 550 (575)	
[Ni(**3**)]$_2$	DMF	292 (6690); 308 (sh); 340 (sh); 380 (sh); 441 (840); 546 (560)	
[Ni(**4**)]$_2$	DMF	290 (6240); 313 (5280); 343 (sh); 378 (1930); 447 (765); 545 (540)	
[Ni(**5**)]$_2$	DMF	290 (7860); 313 (sh); 344 (sh); 380 (sh); 442 (sh); 550 (620)	
[Ni(**6**)]$_2$	DMF	277 (6780); 308 (8140); 387 (1260); 511 (1220)	
[Ni(**1**)CN]$^-$	DMF	275 (18 700); 312 (7530); 432 (661)	
	CH_3CN	273 (24 800); 311 (8620); 419 (485)	
	MeOH	271 (16 800); 305 (6880); 418 (300)	
[Ni(**2**)CN]$^-$	DMF	274 (17 500); 313 (7610); 425 (611)	
	CH_3CN	273 (17 800); 313 (6910); 422 (425)	
	CH_2Cl_2	277 (14 440); 315 (5660); 383 (sh); 405 (425)	
[Ni(**3**)CN]$^-$	DMF	273 (22 500); 313 (6770); 432 (468)	
[Ni(**4**)CN]$^-$	DMF	275 (11 600); 314 (6450); 424 (410)	
[Ni(**5**)CN]$^-$	DMF	274 (18 300); 314 (7470); 422 (427)	
[Ni(**6**)CN]$^-$	DMF	280 (20 200); 311 (5650); 422 (1540)	
[Ni(**1-O$_2$**)CN]	DMF	324 (9630); 380 (sh)	312, 418
	CH_3CN	264 (15 100); 325 (11 100); 389 (sh)	306, 425, 458
[Ni(**2-O$_2$**)CN]$^-$	DMF	324 (8670); 387 (sh)	268, 312
	CH_3CN	324 (11 200); 391 (sh)	309
[Ni(**3-O$_2$**)CN]$^-$	DMF	324 (8830); 389 (sh)	314, 420
[Ni(**4-O$_2$**)CN]$^-$	DMF	324 (7300); 387 (sh)	316, 420, 472
[Ni(**5-O$_2$**)CN]$^-$	DMF	326 (8550); 393 (sh)	318, 430, 460
	CH_3CN	265 (13 700); 325 (8300); 385 (sh)	
[Ni(**6-O$_2$**)CN]$^-$	DNF	276 (7980); 325 (3610)	277, 288, 585
	CH_3CN	275 (7800); 323 (3480)	

[a] Calculated per Ni. [b] Observed during the oxidation of $[Ni(L)CN]^-$ to $[Ni(L\text{-}O_2)CN]^-$.

Table II. Crystallographic Data

compd	Et_4N[Ni(**2**)CN]	Et_4N[Ni(**2-O$_2$**)CN]	Et_4N[Ni(**6**)CN]
formula	$C_{16}H_{35}N_3S_3Ni$	$C_{16}H_{35}N_3O_2S_3Ni$	$C_{13}H_{28}N_2S_3Ni$
fw	424.36	456.36	367.26
cryst system	monoclinic	monoclinic	orthorhombic
space group	$P2_1/c$ (No. 14)[a]	$P2_1/c$ (No. 14)[a]	$P2_12_12_1$ (No. 19)
a (Å)	12.803(8)	12.784(4)	8.871(2)
b (Å)	12.713(9)	12.757(2)	11.505(2)
c (Å)	14.788(12)	14.847(4)	17.767(2)
β (deg)	119.31(6)	115.00(3)	
V (Å^3)	2098.8	2194.5	1813.3
Z	4	4	4
T (°C)	23 ± 2	23 ± 2	23 ± 2
λ (Å)	0.710 73	0.710 73	0.710 73
D_{calc} (g cm^{-3})	1.343	1.381	1.345
μ (cm^{-1})	12.177	11.757	13.973
$R(F_o)$[b]	0.087	0.033	0.044[c]
$R_w(F_o)$[b]	0.106	0.042	0.064[c]

[a] Isomorphous. [b] $R = \sum||F_o| - |F_c||/\sum|F_o|$ and $R_w = \{\sum w(|F_o| - |F_c|)^2/\sum w|F_o|^2\}^{1/2}$. [c] Values are for the configuration with the lowest R_w.

Table III. Selected Atomic Coordinates and B_{eq} Values (Å^2) for $[Et_4N]$[Ni(**2**)CN][a]

atom[b]	x	w	z	B_{eq}[c]
Ni	0.31173(9)	0.09881(9)	0.8977(1)	2.64(3)
S1	0.2268(3)	0.0776(2)	0.7302(2)	4.56(8)
S2	0.3950(2)	0.1259(2)	1.0639(2)	3.91(7)
S3	0.4262(3)	0.5094(2)	0.8685(3)	4.56(9)
N1	0.1348(8)	−0.0448(8)	0.9085(8)	6.0(3)
N2	0.4362(6)	0.1830(5)	0.8944(6)	2.4(2)
C1	0.2005(7)	0.0132(8)	0.9028(8)	3.3(3)
C2	0.4544(8)	0.1473(7)	0.8081(8)	3.4(3)
C3	0.340(1)	0.1408(8)	0.7083(9)	4.5(3)
C4	0.5500(8)	0.1716(8)	0.9946(8)	3.6(3)
C5	0.5318(9)	0.1907(8)	1.0850(9)	4.2(3)
C6	0.3941(7)	0.2971(8)	0.8782(7)	2.5(2)*
C7	0.4788(8)	0.3745(8)	0.8719(7)	3.4(2)*
C8	0.307(1)	0.5197(9)	0.7376(9)	4.6(3)

[a] Numbers in parentheses are estimated standard deviations. [b] Atoms are labeled to agree with Figure 1. [c] Equivalent isotropic thermal parameters are calculated as $(4/3)[a^2\beta_{11} + b^2\beta_{22} + c^2\beta_{33} + ab(\cos\gamma)\beta_{12} + ac(\cos\beta)\beta_{13} + bc(\cos\alpha)\beta_{23}]$.

range for planar Ni thiolate complexes (2.16–2.21 Å).[15] The two values for the Ni–$S_{thioether}$ bond length in [Ni(**6**)CN]$^-$ are indistinguishable from the distances observed for thiolate S-donor atoms.

Reaction of solutions of $Et_4N[Ni(L)CN]$ with O_2 lead to the formation of red-orange solutions from which the yellow to red colored oxygenated products, $Et_4N[Ni(L\text{-}O_2)CN]$, may be isolated. Once bound, the dioxygen cannot be displaced by bubbling N_2 through the mixture and does not exchange with O_2 in the gas phase (vide infra), indicating that the reaction is irreversible. That the Ni is an essential component is indicated by the fact that the ligands do not react to form sulfinates in DMF in the presence or absence of Et_3N (no S–O vibrations are observed in the products). Thus, the reaction involves either activation of O_2 or a thiolate ligand by Ni.

Oxygen uptake measurements demonstrate that the reaction proceeds via the reaction of a single molecule of oxygen per $[Ni(L)CN]^-$ complex (Table VII), and that it is a general feature of the chemistry of these Ni thiolate complexes. Characterization of these products shows that only one of the thiolate ligands can be converted to a sulfinate ligand under these conditions.

The electronic absorption spectra of the oxidized products are characterized by absorbances near 265, 325, and 390 nm (Table I). The 265 nm band is below the spectral window permitted by DMF solutions, but may be observed in CH_3CN solutions. Because Ni complexes of CN^- [16] or RS^- and complexes containing sulfinate ligands all exhibit absorptions in the 400–270 nm range, it is difficult to make specific assignments of the absorptions in the spectra observed for $[Ni(L)CN]^-$ and $[Ni(L\text{-}O_2)CN]^-$. Similar spectra are observed for Co(III) alkyl thiolate complexes and their oxidation products.[17-19]

---

(15) Krüger, H.-J.; Holm, R. H. *Inorg. Chem.* **1989**, *28*, 1148.

(16) (a) Lever, A. B. P. *Inorganic Electronic Spectroscopy*, 2nd ed.; Elsevier: New York, 1984; pp 318, 339. (b) Mason, W. R.; Gray, H. B. *J. Am. Chem. Soc.* **1968**, *90*, 5721.

(17) Sloan, C. P.; Krueger, J. H. *Inorg. Chem.* **1975**, *14*, 1481.

(18) Heeg, M. J.; Elder, R. C.; Deutsch, E. *Inorg. Chem.* **1979**, *18*, 2036.

Table IV. Selected Atomic Coordinates and B_{eq} Values (Å^2) for [Et$_4$N][Ni(**6**)CN]^a

atom^b	x	w	z	B_{eq}^{c}
Ni	0.2410(1)	0.9990(1)	0.83444(6)	4.86(2)
S1	0.3340(4)	1.1739(2)	0.8324(2)	6.76(7)
S2	0.1431(4)	0.8278(3)	0.8284(2)	6.98(8)
S3A	0.3149(5)	0.9847(4)	0.7188(2)	4.47(9)
S3B	0.1802(7)	1.0169(5)	0.7146(3)	5.1(1)
N1	0.2179(7)	0.9982(7)	1.0029(4)	5.8(2)
C1	0.2263(8)	1.0026(9)	0.9388(5)	4.5(2)
C2	0.364(2)	1.2035(9)	0.7347(5)	10.3(5)
C3	0.311(1)	1.127(1)	0.6844(5)	9.3(3)
C4	0.143(2)	0.787(1)	0.7267(6)	9.5(4)
C5	0.187(2)	0.885(1)	0.6804(7)	9.5(4)

^{a} Numbers in parentheses are estimated standard deviations. ^{b} Atoms are labeled to agree with Figure 2. ^{c} Equivalent isotropic thermal parameters are calculated as $(4/3)[a^2\beta_{11} + b^2\beta_{22} + c^2\beta_{33} + ab(\cos\gamma)\beta_{12} + ac(\cos\beta)\beta_{13} + bc(\cos\alpha)\beta_{23}]$.

Table V. Selected Atomic Coordinates and B_{eq} Values (Å^2) for [Et$_4$N][Ni(**2-O$_2$**)CN]^a

atom^b	x	y	z	B_{eq}^{c}
Ni	0.32346(4)	0.09264(3)	0.89499(3)	2.994(9)
S1	0.38508(9)	0.12047(8)	1.05358(7)	4.20(2)
S2	0.27306(8)	0.05971(8)	0.74074(7)	4.11(2)
S3	0.4113(1)	0.50994(8)	0.86912(8)	4.94(3)
O1	0.3079(3)	−0.0470(2)	0.7264(2)	5.89(8)
O2	0.1590(3)	0.0886(3)	0.6714(2)	6.8(1)
N1	0.1406(3)	−0.0516(3)	0.8984(3)	6.1(1)
N2	0.4443(2)	0.1870(2)	0.8925(2)	3.08(6)
C1	0.2096(3)	0.0042(3)	0.8965(3)	3.85(9)
C2	0.5480(3)	0.1779(3)	0.9899(3)	4.2(1)
C3	0.5172(4)	0.1930(3)	1.0766(3)	4.6(1)
C4	0.4760(3)	0.1550(3)	0.8100(3)	3.88(9)
C5	0.3710(3)	0.1440(3)	0.7139(3)	4.5(1)
C6	0.3939(3)	0.2956(3)	0.8775(3)	3.26(8)
C7	0.4709(3)	0.3819(3)	0.8674(3)	4.1(1)
C8	0.2990(4)	0.5157(4)	0.7475(3)	6.1(1)

^{a} Numbers in parentheses are estimated standard deviations. ^{b} Atoms are labeled to agree with Figure 1. ^{c} Equivalent isotropic thermal parameters are calculated as $(4/3)[a^2\beta_{11} + b^2\beta_{22} + c^2\beta_{33} + ab(\cos\gamma)\beta_{12} + ac(\cos\beta)\beta_{13} + bc(\cos\alpha)\beta_{23}]$.

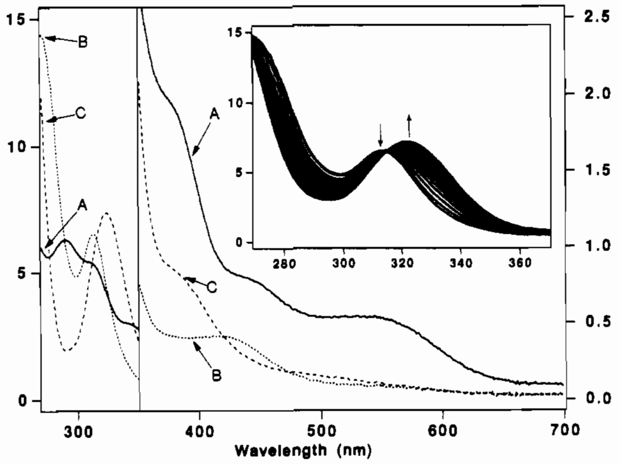

Figure 3. Electronic absorption spectra of [Ni(**4**)]$_2$ (A), Et$_4$N[Ni(**4**)CN] (B), and Et$_4$N[Ni(**4-O$_2$**)CN] (C) in DMF. The inset describes spectral changes occurring in the UV region during reaction of Et$_4$N[Ni(**4**)CN] with O$_2$. Extinction coefficients are for a constant [Ni] = 2.00 mM.

Table VI. Selected Bond Lengths (Å) and Angles (deg)

bond or angle	[Ni(**2**)CN]$^-$	[Ni(**2-O$_2$**)CN]$^-$	[Ni(**6**)CN]$^-$ (A)
		Bonds	
Ni–S1	2.180(3)	2.173(1)	2.175(3)
Ni–S2	2.175(3)	2.146(1)	2.156(3)
Ni–N2 (S3)	1.940(8)	1.970(3)	2.162(4)
Ni–C1	1.82(1)	1.849(4)	1.859(8)
S1–C3 (C2)	1.82(1)	1.828(4)	1.79(1)
S2–C5 (C4)	1.82(1)	1.816(5)	1.87(1)
S2–O1		1.474(3)	
S2–O2		1.432(3)	
C1–N1	1.15(2)	1.143(6)	1.14(1)
		Angles	
S1–Ni–S2	177.9(1)	176.21(5)	175.9(1)
S1–Ni–N2 (S3)	89.9(3)	89.56(9)	86.5(1)
S1–Ni–C1	90.5(3)	90.8(1)	91.3(3)
S2–Ni–N2 (S3)	89.2(2)	89.04(9)	90.3(1)
S2–Ni–C1	90.5(3)	90.6(1)	92.4(3)
N2–Ni–C1	176.7(4)	179.6(1)	166.0(3)
Ni–S1–C3 (C2)	98.6(4)	99.7(1)	104.3(4)
Ni–S2–C5 (C4)	99.5(4)	101.1(1)	106.2(4)
Ni–S2–O1		111.1(1)	
Ni–S2–O2		118.1(2)	
O1–S2–O2		114.4(2)	
O1–S2–C5		103.8(2)	
O2–S2–C5		106.2(2)	
Ni–C1–N1	176.4(9)	178.8(3)	176.1(9)

Spectral changes that occur upon oxidation of [Ni(L)CN]$^-$ to [Ni(L-O$_2$)CN]$^-$ invariably involve the shift of the absorbance near 275 nm in [Ni(L)CN]$^-$ to shorter wavelengths. Oxidation of [Ni(L)CN]$^-$ is also accompanied by the shift of the band near 310 nm to 325 nm. These changes are illustrated for the oxidation of [Ni(**4**)CN]$^-$ in Figure 3. Similar spectra have been reported previously for [Ni(**2**)CN]$^-$ and [Ni(**2-O$_2$**)CN]$^-$.[7]

The spectra of [Ni(L)CN]$^-$ complexes do not change over a 24 h period under N$_2$, but slowly convert to the spectra characteristic of [Ni(L-O$_2$)CN]$^-$ in the presence of O$_2$. These spectra reveal clear isosbestic points in every case, indicating that no stable intermediate builds up in the conversion of [Ni(L)CN]$^-$ to [Ni(L-O$_2$)CN]$^-$. The planar diamagnetic complexes feature a single S-bonded sulfinato ligand, which gives rise to three characteristic vibrations in the IR spectra: $\nu_a(SO_2)$ near 1170 cm^{-1}, $\nu_s(SO_2)$ near 1050 cm^{-1}, $\delta(SO_2)$ near 570 cm^{-1}.[20] In the cases of Et$_4$N[Ni(**1-O$_2$**)CN] and Et$_4$N[Ni(**2-O$_2$**)CN], comparison of the spectra obtained from natural abundance O$_2$ with those obtained by using $^{18}O_2$ in the preparation of the complexes has made the unambiguous assignment of bands at 1170, 1045, and 550 cm^{-1} that shift to 1142, 1001, and 525 cm^{-1} in ^{18}O labeled samples of Et$_4$N[Ni(**1-O$_2$**)CN], and bands at 1173, 1047 cm^{-1} that shift to 1131, 1000 cm^{-1} in ^{18}O labeled samples of Et$_4$N[Ni(**2-O$_2$**)CN], to these vibrations. Additional IR spectral data can be found in the Experimental Section.

The structure of crystals of Et$_4$N[Ni(**2-O$_2$**)CN] has been communicated in preliminary form.[7] The final structure is summarized in Figure 1 and Tables II, V and VI. Et$_4$N[Ni(**2-O$_2$**)CN] is isomorphous with Et$_4$N[Ni(**2**)CN]. The most significant differences in the unit cell dimensions which accompany the incorporation of the two O atoms are a 4.3° decrease in the β angle and an increase in the unit cell volume of ca. 96 Å^3. The general features of the geometry of both the anions and cations in the two structures are the same. The Ni center in Et$_4$N[Ni(**2-O$_2$**)CN] is essentially planar, with the Ni and the ligand donor atoms (S1, S2, C1, and N2) coplanar to within ±0.034(3) Å. The Ni–S bond length associated with the remaining thiolate S-donor atom is essentially unchanged from those observed in [Ni(**2**)CN]$^-$. The Ni–S bond length associated with the sulfinate S donor atom (2.146(1) Å) is slightly shorter than other Ni–S bond lengths observed in these compounds.

Reaction Kinetics. Kinetic data for the oxidations of [Ni(L)CN]$^-$ complexes are collected in Table VII, and show that the oxidation reaction is first order in [Ni] and in [O$_2$]. The oxidations obey the rate law: $d[[Ni(L\text{-}O_2)CN]^-]/dt = k[[Ni(L)CN]^-][O_2]$. Pseudo-first-order rate constants were measured

---

[19] Lange, B. A.; Libson, K.; Deutsch, E.; Elder, R. C. *Inorg. Chem.* **1976**, *15*, 2985.

[20] (a) Vitzthum, G.; Lidner, E. *Angew. Chem., Int. Ed. Engl.* **1971**, *10*, 315. (b) Lidner, E.; Lorenz, I.-P. *Chem. Ber.* **1972**, *105*, 1032.

Table VII. Kinetic Data and Oxygen Uptake Measurements

complex	rxn solvent	$p(O_2)$ (atm)	T (°C)	k_{obs}[b] (10^4 s^{-1})	k[c] (10^2 M^{-1} s^{-1})	$t_{1/2}$ (h)	no. of half-lives[d] (h)	ΔH^{*}[f] (kcal/mol)	ΔS^{*}[f] (e.u.)	O_2/Ni (uptake)
[Ni(**1**)CN]	DMF	1.0	30	1.05(1)	2.05	1.83	2.2	13.8	−21.3	0.92
			40	1.93(1)	4.17	1.00	5.0			
			50	3.81(1)	8.92	0.51	4.9			
		1.0	30	1.02(2)	1.99	1.88	0.9			
		0.80		0.80(5)	1.95	2.4	0.6			
		0.60		0.60(4)	1.95	3.2	0.5			
		0.40		0.40(4)	1.95	4.8	0.3			
		0.20		0.20(3)	1.95	9.6	0.2			
	CH_3CN	1.0		0.20(1)		9.6	2.8			
	MeOH			N.R.			(24)[e]			
	0.2 M TB in DMF[a]			1.05(1)		1.84	3.8			
[Ni(**2**)CN]	DMF	1.0	30	0.85(2)	1.66	2.27	3.1	14.7	−18.7	0.99
			40	1.69(1)	3.65	1.14	3.5			
			50	3.39(2)	7.94	0.57	3.8			
		1.0	30	0.85(9)	1.66	2.3	0.7			
		0.80		0.68(12)	1.66	2.8	0.6			
		0.60		0.51(8)	1.66	3.8	0.4			
		0.40		0.33(10)	1.61	5.8	0.3			
		0.20		0.17(7)	1.66	11.	0.1			
	CH_3CN	1.0		0.24(2)		8.0	3.1			
	0.02 M TBP in DMF[a]			0.92(13)		2.1	3.6			
	4.0 mM dabco in DMF[a]			1.20(1)		1.6	3.1			
[Ni(**3**)CN]	DMF	1.0	30	0.81(7)	1.58	2.4	3.7	13.5	−22.5	0.93
			40	1.52(1)	3.28	1.27	4.6			
			50	2.89(2)	6.77	0.67	6.0			
[Ni(**4**)CN]	DMF	1.0	30	0.72(2)	1.41	2.7	3.4	13.1	−24.2	
			40	1.45(1)	3.13	1.33	4.0			
			50	2.83(3)	6.63	0.68	5.9			
[Ni(**5**)CN[	DMF	1.0	30	1.60(1)	3.13	1.2	5.8			
[Ni(**6**)CN]	DMF	1.0	30	0.35(18)	0.7	5.5	4.6			1.04

[a] TB = 4-*t*-butylphenol; TBP = 2,4,6-tri-*t*-butylphenol; dabco = 1,4-diazabicyclo[2.2.2]octane. [b] Errors indicated for the rates of reaction were estimated from the fits of the data. [c] k was calculated using $k = K_{obs}/[O_2]$. [d] The reactions were followed for the number of half-lives indicated. For determination of the dependence of the rate on $[O_2]$, the reactions were followed for 100 min. [e] Number of hours withour reaction. [f] Calculated from the equation $k = (k^{*}T/h) \exp(\Delta S^{*}/R) \exp(-\Delta H^{*}/RT)$; where k = the second order rate constant, k^{*} = Boltzman constant, h = Plank's constant.

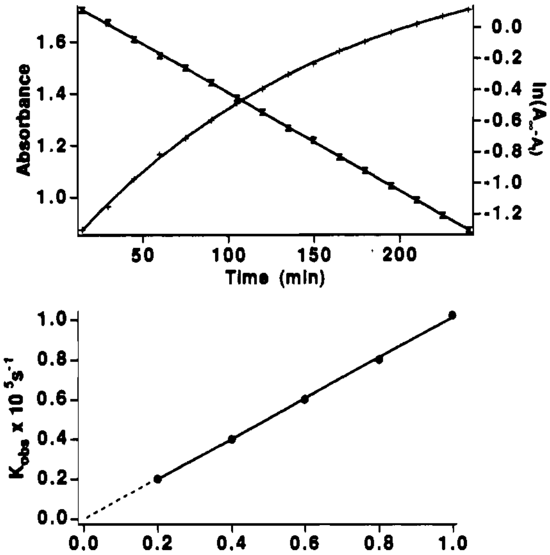

Figure 4. Kinetic data and fits of the oxidation of $Et_4N[Ni(\mathbf{1})CN]$ in DMF at 30°. Top: Changes in A_{325} with time. Bottom: Oxygen dependence of the reaction rate at 30°.

under constant $[O_2]$ and vary from (0.3–1.6) × 10^{-4} s^{-1} at 1 atm of O_2 and 30° for the complexes examined.[21] The data for the oxidation of $[Ni(\mathbf{1})CN]^-$ is shown graphically in Figure 4. The only product of the oxidation reaction is $[Ni(L\text{-}O_2)CN]^-$ and no evidence for the formation of any other product (e.g. bis-sulfinato or disulfides) exists. The spectra recorded during kinetic runs display isosbestic points and the final spectrum is identical to those obtained from isolated, analytically pure product in every case. The pseudo-first-order rate constants display little sensitivity to the nature of the N-substituent. In contrast, the oxidation is very sensitive to the presence of the N-donor atom. The oxidation of $[Ni(\mathbf{6})CN]^-$, which contains a thioether S-donor in place of the N-donor, oxidizes at a rate 2–5 times slower than complexes with N-donor ligands.

The oxidations are solvent dependent, and show a decrease in the rate in the order DMF > CH_3CN > MeOH (Table VII). The reactions show the same spectral changes in CH_3CN as in DMF, indicating that the reaction follows the same course in the two solvents. However, the rate of reaction is 3.5–5.0 times slower in CH_3CN. Although $[Ni(\mathbf{1})]_2$ reacts with $Et_4N(CN)$ in MeOH, as evidenced by the appropriate spectral changes, no oxidation of $[Ni(\mathbf{1})CN]^-$ was observed over a period of 24 h.

The activation parameters ΔH^{*}, and ΔS^{*} were measured using the temperature dependence of the second-order rate constants in DMF, and are compiled in Table VII. The values of ΔH^{*} measured range from 13.1–14.7 kcal/mol. Values of ΔS^{*} range from −24.2 to −18.7 e.u. and are all negative, a characteristic reflecting the loss of rotational and translational degrees of freedom of small molecules upon "coordination".[22] All of the parameters are essentially the same, and indicate the same reaction path is followed for all of the complexes.

For $[Ni(\mathbf{1})CN]^-$ and $[Ni(\mathbf{2})CN]^-$, the dependence of the rate on the $[O_2]$ was measured (Figure 4, Table VII). In both cases, a plot of $\log[O_2]$ vs $\log k_{obs}$ gives a straight line with a slope equal

---

(21) The units in the previously reported rate constant (ref 7) are in error and should be min^{-1} rather than s^{-1}.

(22) Chen, D.; Martell, A. E. *Inorg. Chem.* **1987**, *26*, 1026.

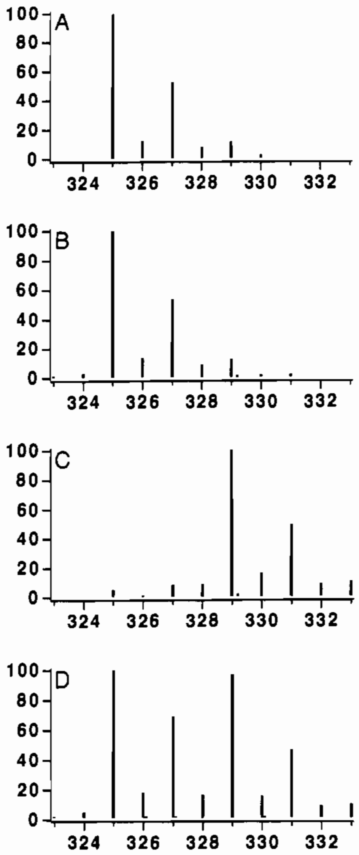

Figure 5. Negative ion FAB mass spectra of Et$_4$N[Ni(**2**-O$_2$)CN]: (A) Theoretical spectrum for [Ni(**2**-^{16}O$_2$)CN$^-$; (B) experimental spectrum of [Ni(**2**-^{16}O$_2$)CN]$^-$; (C) experimental spectrum of [Ni(**2**-^{18}O$_2$)CN]$^-$; (D) spectrum of the oxidation products obtained from a 54% ^{16}O$_2$, 46% ^{18}O$_2$ gas mixture.

to 1.00. Given the solubility of O$_2$ in DMF,[23] second order rate constants of (1.4–3.1) $\times$ 10^{-2} M^{-1} s^{-1} were obtained for the amine ligands, and 0.7 $\times$ 10^{-2} M^{-1} s^{-1} was obtained for the thioether ligand.

No evidence for involvement of radicals (e.g. RS$^\bullet$, O$_2^-$) or for Ni(III) intermediates was obtained. Oxidations monitored by EPR did not display any EPR signals. Further, the pseudo-first-order rate constants for the oxidations of [Ni(**1**)CN]$^-$ and [Ni(**2**)CN]$^-$ in DMF did not show a dependence on the presence of the radical scavengers 4-*t*-butyl phenol and 2,4,6-tri-*t*-butyl phenol (Table VII). Similarly, no evidence for the involvement of singlet O$_2$ was observed. Reactions carried out in the presence of 1,4-diazabicyclo[2.2.2]octane, a singlet O$_2$ scavenger,[24] did not show an effect on the rate of the oxidation reaction.

Isotopic Labeling Studies. Reactions using ^{18}O$_2$ were undertaken in order to investigate the source of oxygen and ascertain if both atoms of oxygen in the product are derived from the same O$_2$ molecule. FAB-mass spectra of various reaction products are shown in Figures 5 and 6. Oxidation of [Ni(**2**)CN]$^-$ in DMF under an ^{18}O$_2$ atmosphere (97–98%) yields only dilabeled product within the purity of the ^{18}O$_2$ used. This indicates that all of the oxygen in the product is derived from O$_2$ and not from the reaction solvent (DMF) or trace water.

Reactions of [Ni(**1**)CN]$^-$ and [Ni(**2**)CN]$^-$ were also conducted under mixtures of ^{16}O$_2$ and ^{18}O$_2$ and analyzed by FAB mass spectroscopy. In the case of [Ni(**1**)CN]$^-$, the complex was labeled with 99.9% ^{58}Ni in order to simplify the mass spectral analysis.

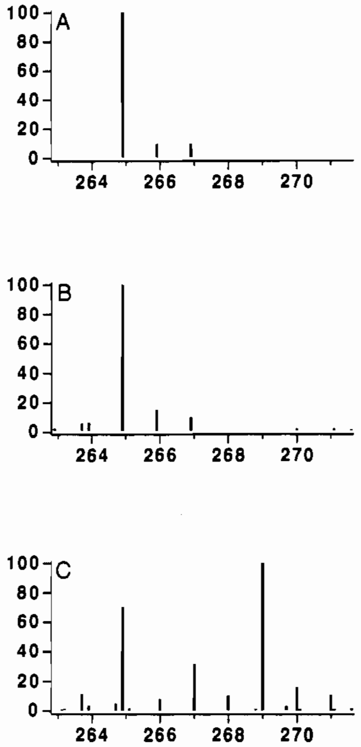

Figure 6. Negative ion FAB mass spectra of Et$_4$N[^{58}Ni(**1**-O$_2$)CN]: (A) Theoretical spectrum for [^{58}Ni(**1**-^{16}O$_2$)CN]$^-$; (B) experimental spectrum of [^{58}Ni(**1**-^{16}O$_2$)CN]$^-$; (C) spectrum of the oxidation products obtained from a 41% ^{16}O$_2$, 59% ^{18}O$_2$ gas mixture.

[^{58}Ni(**1**)CN]$^-$ was exposed to high purity ^{16}O$_2$ and to a mixture of 59% ^{18}O$_2$ and 41% ^{16}O$_2$. These spectra are compared in Figure 6, along with a theoretical spectrum derived from the contributions of the natural abundance of isotopes of C, N, and S. The theoretical spectrum of [^{58}Ni(**1**-^{16}O$_2$)CN]$^-$ is dominated by the parent ions containing only ^{58}Ni, ^{16}O and the most abundant stable isotopes of C, H, N, and S (mass = 265). Two other peaks with intensity >1% are observed. The first is due to parent ions containing one ^{13}C, ^{15}N, ^{33}S, or ^{2}H (266, 9.16%). The second is derived principally from anions containing one ^{34}S (267, 9.24%). The experimental spectrum (265, 100%; 266, 14.98%, and 267, 9.98%) is in agreement with the theoretical spectrum. For the product derived from the gas mixture, two limiting cases were considered. In the first case, a single molecule of O$_2$ provides both O atoms in the product. If this is a feature of the reaction mechanism, only masses 265 and 269 would be observed in the ratio of 41% to 59% after subtraction of the minor contributions from isotopes of C, H, N, and S. Alternatively, if the O atoms in the product are completely scrambled, three masses in a statistical distribution would be observed (265, 17%; 267, 48%; 269, 35%). The result, after subtraction of the minor contributions discussed, reveals all three masses in a non-statistical distribution (265, 37%; 267, 11%; 269, 52%). Clearly, most of the product is derived from the incorporation of both atoms of oxygen from a single O$_2$ molecule.

A similar analysis that also takes into account the contributions from the natural abundance of the stable isotopes of Ni, yields a similar result for [Ni(**2**-O$_2$)CN]$^-$. From a gas mixture containing 54% ^{16}O$_2$ and 46% ^{18}O$_2$, the expected theoretical distribution for complete scrambling of the O isotopes is: 325, 29%; 327, 50%; 329, 21%. The observed corrected distribution is: 325, 50%; 327, 8%; 329, 42%.

Both experiments are consistent with the major reaction path stemming from incorporation of both atoms of oxygen from a single O$_2$ molecule. However, both reactions reveal about 20% of the amount of ^{16}O^{18}O product expected from complete scrambling of the label. One possibility is that the sulfinato O

---

[23] Values for the solubility of O$_2$ in DMF were obtained at T = 15, 30, and 45° (0.1340, 0.1273, and 0.1140 mL/mL, respectively) from: Mirza, S. A., Ph.D. Dissertation, Bhavnagar University, 1989. The solubility at other temperatures was obtained from a Van't Hoff plot.

[24] Ogilby, P. R.; Foote, C. S. *J. Am. Chem. Soc.* **1983**, *105*, 3423.

atoms can exchange slowly with atmospheric O_2. This possibility was checked for $[Ni(\mathbf{1}\text{-}^{16}O_2)]^-$ by dissolving a sample in DMF and stirring it under an atmosphere of $^{18}O_2$ for 8 h, the reaction time used to generate all the labeled samples of $[Ni(\mathbf{1}\text{-}O_2)CN]^-$. The resulting product had a composition of ca. 3% mass 267 and <4% mass 269 over that expected for the starting material. Thus, the oxygenated product does not exchange with O_2 to an appreciable extent. Another possibility involves chemistry occurring in the FAB mass spectrometry experiment. This possibility is ruled out by the fact that a physical mixture of $[Ni(\mathbf{1}\text{-}^{16}O_2)CN]^-$ and $[Ni(\mathbf{1}\text{-}^{18}O_2)CN]^-$ gave a spectrum consistent with no exchange of sulfinate O atoms within an error of 3%. Thus, the 20% amount of $^{16}O^{18}O$ product observed in the product mixture apparently arises from another reaction mechanism, presumably a bimolecular reaction involving the intermediate(s).

Discussion

Mechanistic Insights. Oxidations of thiols, thiolates, and thiolato complexes with O_2 typically form disulfides, presumably via the formation of thiyl radicals.[25] The reactions studied here are unusual in that dioxygen is incorporated into the product. Few examples of such reactions have been observed.[26-28] Recently, a study of the oxidation of a Ni(II) complex with a *cis*-N_2S_2 donor atom set was reported.[28] This work indicated that oxidation of the *cis*-N_2S_2 complex by O_2 led to the formation of three products that were separated by using column chromatography.[28] These products were identified as a monosulfinato complex analogous to the oxidation products described here, a bis-sulfinato complex, and a trinuclear complex derived from reaction of Ni^{2+} with the starting material. The mass spectral results reported for the monosulfinato complex are consistent with those reported here. However, oxidation by O_2 of the trans-dithiolato complexes discussed here result in the formation of only the monosulfinato product. Chromatographic analysis of the reaction mixture obtained from the O_2 oxidation of $[Ni(\mathbf{1}\text{-L})CN]^-$ reveals only a single orange band corresponding to the monosulfinato product.

Preliminary results obtained from the oxidation of an analogous Ni(II) complex with a *cis*-N_2S_2 ligation,[10] confirms the results reported by Farmer et al. in that three products are separated by chromatography; the orange monosulfinate, a yellow compound and a green compound. However, we do not observe any unreacted starting material in the product mixture. This reaction differs from those of the trans-dithiolates studied in detail here in that the O_2 stoichiometry is 2.0:1 Ni and the rate of reaction at 40° in DMF is slower ($1.7 \times 10^{-5}\ s^{-1}$, based on the disappearance of the spectrum of the starting material).

That the monosulfinate is the only product formed in significant amounts from O_2 oxidation of the trans-dithiolato amine complexes is also supported by the facts that the reaction obeys first order kinetics over 3–5 half lives (>97% completion), involves uptake of one O_2 molecule/Ni, and the final spectra are identical to those obtained from isolated, analytically pure products, one of which has been crystallographically characterized.[7]

The only well-characterized mechanism for the oxidation of thiolates to sulfinates in transition metal complexes by dioxygen species involves O_2^{2-} as an oxidant and proceeds via the stepwise formation of sulfenates (Scheme I).[13,29] The reaction mechanism has been interpreted as involving nucleophilic attack of the coordinated thiolate S atom on the peroxide (H_2O_2, $H_3O_2^+$) and follows the rate law: Rate = $k_2[\mathrm{Nuc}][H_2O_2]$. Although the rate law and the kinetic barriers determined for this mechanism in a number of complexes are similar to those observed for the oxidation of $[Ni(L)CN]^-$ (e.g. for $[(en)_2Cr(SCH_2CH_2NH_2)]$: $\Delta H^{\ddagger} = 9.7(2)$ kcal/mol, $\Delta S^{\ddagger} = -26$ e.u.), the stoichiometry of the reactions studied here ($1Ni{:}1O_2$) rules out a stepwise mechanism for the oxidation of $[Ni(L)CN]^-$ complexes. Such a mechanism would also be expected to give rise to complete scrambling of labeled oxygen in reactions involving $^{16}O_2$ and $^{18}O_2$, in contrast to the observation that the oxidation of $[Ni(L)CN]^-$ proceeds mostly with the incorporation of both atoms of a single O_2 molecule.

Scheme I

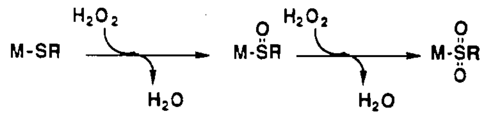

Despite the differences in mechanism, the expectation that thiolate ligands will act as nucleophiles is likely to be a feature of the oxidation of $[Ni(L)CN]^-$ by O_2. The strong tendency of Ni thiolates to form dimers and higher polymers,[10,30] and the fact that the presence of a tightly bound anionic ligand appears to be required to cleave the dinuclear complexes (e.g. CN^- or thiolate[15]) is evidence of the nucleophilicity of terminal thiolate ligands in planar Ni(II) complexes.

Mechanisms involving radicals were also considered. The reaction of thiyl radicals with O_2 is known to form sulfinyl radicals.[31] Although such a mechanism would have the correct stoichiometry and account for the lack of scrambling in the studies involving labeled O_2, reactions involving the formation of free radicals may be ruled out since the rates of reaction are not effected by the presence of radical scavengers.

The ability of transition metals to form complexes with O_2 is well known. Recently, the ability of Ni(II) complexes to reversibly bind O_2 has been characterized.[32,33] The O_2 complexes are powerful oxidizing agents, and have been described as involving formal Ni(III) and O_2^- centers. The formation of a Ni–O_2 complex as a precursor to the ligand oxidation of $[Ni(L)CN]^-$ is unlikely, since the spectrum of $[Ni(\mathbf{1})CN]^-$ taken under 1 atm of O_2 at 15°, a temperature that is below that required to halt the ligand oxidation, is identical to those of anaerobic samples of $[Ni(\mathbf{1})CN]^-$ and does not change in 6 h. Further, no intermediates are detected in the oxidation process. Mechanisms involving the production of free O_2^- via oxidation of the metal center, followed by oxidation of thiolate ligands by the O_2^- (or O_2^{2-} from reaction with a second Ni center) are inconsistent with the lack of EPR signals from Ni(III) and the absence of an effect on the rates of reaction in the presence of radical traps. Further, these reactions would be expected to proceed stepwise, as in Scheme I, leading to the formation of intermediates and to complete scrambling of labeled O_2.

A mechanism that is consistent with the data gathered in this study for the oxidation of $[Ni(L)CN]^-$ by O_2 is shown in Scheme

---

[25] Capozzi, G.; Modena, G. *The Chemistry of the Thiol Group*; Patai, S., Ed.; John Wiley and Sons: New York, 1974; Chapter 17.

[26] Schrauzer, G. N.; Zhang, C.; Chadha, R. *Inorg. Chem.* **1990**, *29*, 4104.

[27] (a) Nicholson, T.; Zubieta, J. *Inorg. Chem.* **1987**, *26*, 2094. (b) Thompson, J. S.; Marks, T. J.; Ibers, J. A. *J. Am. Chem. Soc.* **1979**, *101*, 4180.

[28] Farmer, P. J.; Solouki, T.; Mills, D. K.; Soma, T.; Russel, D. H.; Reibenspies, J. H.; Darensbourg, M. Y. *J. Am. Chem. Soc.* **1992**, *114*, 4601.

[29] Deutsch, E.; Root, M. J.; Nosco, D. L. *Adv. Inorg. Bioinorg. Mech.* **1982**, *1*, 269.

[30] (a) Nicholson, J. R.; Christou, G.; Huffman, J. C.; Folting, K. *Polyhedron* **1987**, *6*, 863. (b) Tremel, W.; Kriege, M.; Krebs, B.; Henkel, G. *Inorg. Chem.* **1988**, *27*, 3886. (c) Kriege, M.; Henkel, G. Z. *Naturforsch.* **1987**, *42B*, 1121.

[31] (a) Chatgilialoglu, C.; Guerra, M. *Sulfur-Centered Reactive Intermediates in Chemistry and Biology*; Chatgilialoglu, C., Asmus, K-D., Eds.; Plenum Press: New York, 1990; p 31. (b) Griller, D.; Simões, J. A. M. *Sulfur-Centered Reactive Intermediates in Chemistry and Biology*, *Ibid.*, p 327.

[32] (a) Kimura, E.; Sakonaka, A.; Machida, R. *J. Am. Chem. Soc.* **1982**, *104*, 4255. (b) Kimura, E.; Machida, R. *J. Chem. Soc., Chem. Commun.* **1984**, 499. (c) Kushi, Y.; Machida, R.; Kimura, E. *J. Chem. Soc., Chem. Commun.* **1985**, 216. (d) Kimura, E.; Anan, H.; Toike, T.; Shiro, M. *J. Org. Chem.* **1989**, *54*, 3998. (e) Kimura, E.; Sakonaka, A.; Machida, R. *J. Am. Chem. Soc.* **1982**, *104*, 4255. (f) Machida, R.; Kimura, E.; Kushi, Y. *Inorg. Chem.* **1986**, *25*, 3461.

[33] Chen, D.; Motekaitis, R. J.; Martell, A. E. *Inorg. Chem.* **1991**, *30*, 1396.

Scheme II

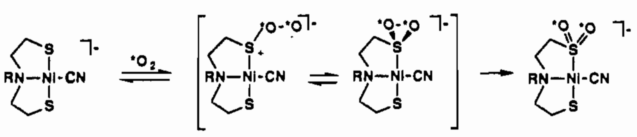

II. A successful mechanism for this reaction must (1) account for the stoichiometry of the reaction, (2) have a major pathway involving incorporation of both atoms of a single O_2 molecule, and (3) feature a rate-determining step that involves one Ni complex and one O_2 molecule.

The proposed mechanism involves the formation of persulfoxide and thiadioxirane intermediates. These intermediates have been suggested to be involved in the oxidation of thioethers by $^1O_2$[34–36] and have been postulated for the oxidation of Ni dithiolenes to bis-sulfinates.[26] (In contrast to the dithiolene oxidation, strong basic conditions are not involved in the oxidations of [Ni(L)CN]$^-$.) The mechanism of thioether oxidation is described as involving electrophilic attack of $^1O_2$ on the sulfur atom (or conversely nucleophilic attack of thioether S on $^1O_2$) and leads to the formation of sulfoxides and sulfones. Further, a recent study employing $^{18}O_2$ revealed that the product sulfone contains two atoms of oxygen *derived from the same O_2 molecule*.[34] Since addition of the $^1O_2$ scavenger DABCO has no effect on the rate of reaction (Table VII), singlet oxygen is not directly involved. However, nucleophilic attack of the coordinated thiolates on $^3O_2$ does account for the stoichiometry of the reaction, the derivation of the major product from a single O_2 molecule, the absence of radical intermediates, and does not involve Ni-centered redox chemistry. It is possible that the increased nucleophilicity of thiolate sulfur vs thioether sulfur[37] is enough to cause the reaction to occur, albeit slowly, with the weaker electrophile.

The rate determining step in the proposed mechanism is the cleavage of the O–O bond in the thiadioxirane intermediate. This conclusion is based on the similarity between the enthalpy and entropy of activation for a number of oxidations where O–O bond cleavage is rate determining (e.g. Scheme I). However, given the absence of detectable intermediates in the reaction and the extremely short-lived nature of organic thiadioxirane and persulfoxide species, it is possible that the formation of the thiadioxirane intermediate is rate determining and has coincidentally similar activation parameters.

Since no scrambling of the oxygen label is observed in the monosulfinate products, any reaction leading to scrambling of this label must occur before the product is formed. One possibility for the formation of products containing both ^{16}O and ^{18}O involves a bimolecular reaction of the ring-open form (persulfoxide) of the intermediate with either another such intermediate or a dithiolate complex. In any event, these minor bimolecular reactions cannot involve the rate-determining step, since the kinetics are first order in [Ni] and show no deviation at higher concentrations, where bimolecular reaction intermediates would be more favored.

The reaction of only one thiolate, the dependence of the rate of reaction on the nature of the ligand donor atom set, and the solvent dependence observed for the reaction can be explained in terms of a mechanism involving nucleophilic attack by a thiolate ligand on O_2. Nucleophilic substitution reactions in general proceed more rapidly in DMF than in MeOH, as is the case for reactions of Co(III) thiolates.[38] This is consistent with the generalization that in a reaction where the reactants have a higher charge density than the transition state (i.e. thiolato vs sulfinato S atoms), the reaction will proceed more rapidly as the solvent polarity decreases. The differences in rates cannot be traced to the solubility of O_2 in the solvents used, since the [O_2] in CH_3CN is greater than in DMF.[39,40] It also appears unlikely that changes in ion pairing effects mediated by the solvent dielectric constants are involved, since reaction rates measured in the presence of a 10-fold excess of Et_4NCl in DMF and CH_3CN are unaffected by the presence of an excess of Et_4N^+. Thus, the solvent dependence of the rate of oxidation (DMF > CH_3CN > MeOH) reflects the increasing polarity ($Z_{\mathrm{DMF}} = 68.5$, $Z_{\mathrm{CH_3CN}} = 71.3$, $Z_{\mathrm{MeOH}} = 83.6$)[41] of the solvents.

Although the [Ni(L)CN]$^-$ complexes contain two chemically identical thiolate ligands, only one of them reacts with O_2 under the conditions explored. Because the oxidized S center would be expected to be a poorer electron-donor than thiolate S, the thiolates in [Ni(L)CN]$^-$ are more electron rich than the one that remains in [Ni(L-O_2)CN]$^-$. This is because the Ni (II) center would be expected to increase in Lewis acidity upon oxidation of the first thiolate, causing a loss of electron density from the remaining thiolate ligand. With less electron density, the remaining thiolate is less nucleophilic and should react with O_2 with less facility.

Comparison of the rates of the oxidations of [Ni(**1–5**)CN]$^-$ and [Ni(**6**)CN]$^-$ lead to the same conclusion. The rate of oxidation of [Ni(**6**)CN]$^-$ is 2–3 times slower than for the tertiary amine containing ligands. The thioether donor in [Ni(**6**)CN]$^-$ is expected to be a poorer σ-donor than the tertiary amine N-donor in [Ni(**1–5**)CN]$^-$.[42] This in turn increases the Lewis acidity of the Ni center in [Ni(**6**)CN]$^-$ and results in thiolate ligands that would be expected to have reduced nucleophilicity. These trends are in agreement with a recent study of inductive effects on the rate of oxidation of Ru(III) complexes with substituted thiophenolate ligands to Ru(III) sulfenato complexes.[43]

A similar argument for the difference in the reactivity between the cis- and trans-dithiolato complexes can be advanced. Oxidation of a trans-thiolate ligand would be expected to have a greater influence on the reactivity of the remaining thiolate ligand than oxidation of a cis-thiolate ligand. It is also likely that the oxidation mechanism differs significantly between cis- and trans-dithiolates. Nonetheless, the observation of the oxidation of alkyl thiolate ligands leading to the formation of sulfinate products in a variety of Ni complexes has important implications for corresponding cysteinate oxidations in Ni enzymes, and possibly for the oxidation of cysteinate ligands in metalloenzymes in general.

Biological Insights. One biological route for the oxidative metabolism of cysteine leads to the formation of a number of oxy acid intermediates, such as cysteine sulfenic acid, cysteine sulfinic acid, 2-aminoethanesulfinic acid (hypotaurine), cysteine sulfonic acid (cysteic acid), and 2-aminoethanesulfonic acid (taurine).[44] Taurine is an important biological product of cysteine metabolism that is involved in a number of biological processes.[44] Cysteine sulfinic acid (CSA) is a key intermediate in the synthesis of taurine, and is synthesized from cysteine and O_2 in the liver by the enzyme cysteine dioxygenase. Cysteine dioxygenase is an Fe containing metalloenzyme that inserts both atoms of dioxygen into the product.[45] Similar results have been obtained for the enzymatic

---

(34) Watanabe, Y.; Kuriki, N.; Ishiguro, K.; Sawaki, Y. *J. Am. Chem. Soc.* **1991**, *113*, 2677.

(35) Akasaka, T.; Haranaka, M.; Ando, W. *J. Am. Chem. Soc.* **1991**, *113*, 9898.

(36) Liang, J.-J.; Gu, C.-L.; Kacher, M. L.; Foote, C. S. *J. Am. Chem. Soc.* **1983**, *105*, 4717.

(37) Ashby, M. T. *Comments Inorg. Chem.* **1990**, *10*, 297.

(38) Root, M. J.; Deutsch, E. *Inorg. Chem.* **1981**, *20*, 4376.

(39) [O_2] in CH_3CN at 25° = 8.1 mM: Sawyer, D. T.; Chiericato, G., Jr.; Angelis, C. T.; Nanni, E. J., Jr.; Tsuchiya *Anal. Chem.* **1982**, *54*, 1720.

(40) [O_2] in MeOH at 18.8° = 7.3 mM: *Int. Critical Tables Numerical Data* **1928**, *3*, 255.

(41) Drago, R. S. *Physical Methods in Chemistry*; W. B. Saunders: Philadelphia, PA, 1977; p 122.

(42) (a) Jørgensen, C. K. *Prog. Inorg. Chem.* **1970**, *12*, 101. (b) Jørgensen, C. K. *Inorg. Chim. Acta Rev.* **1968**, *2*, 65.

(43) Johnson, M. D.; Nickerson, D. *Inorg. Chem.* **1992**, *31*, 3971.

(44) Huxtable, R. J. *Biochemistry of Sulfur*; Plenum Press: New York, 1986; Chapter 4.

(45) Lombardini, J. B.; Singer, T. P.; Boyer, P. D. *J. Biol. Chem.* **1969**, *244*, 1172.

oxidation of cysteamine to hypotaurine.[46] The mechanism postulated for the oxidation of a 2-amino thiolate in $[Ni(L)CN]^-$ may well mimic these biological oxidations.

Experimental Section

Preparation of Compounds. All solvents were dried by using conventional methods and distilled and stored under N_2 atmosphere. Except where noted, starting materials were of reagent grade and were obtained from the commercial sources indicated. The 2,4,6-tri-*t*-butylphenol (Aldrich) was sublimed prior to use. All synthetic procedures involving manipulations of solutions of the ligands and their Ni complexes were carried out under an N_2 atmosphere by using standard Schlenk techniques unless otherwise noted. Samples submitted for microanalysis were routinely ground to a fine powder and vacuum desiccated over P_4O_{10} overnight prior to analysis.

Bis(2-mercaptoethyl)methylamine Hydrochloride (1·HCl). Bis(2-chloroethyl)methylamine hydrochloride (9.76 g, 50.6 mmol) (Aldrich) was dissolved in EtOH (36 mL) and thiourea (8.10 g, 106.6 mmol) (Aldrich) was added. The solution was refluxed for 4.5 h. Upon cooling a gummy solid formed. Dry HCl gas was bubbled through the solution and the contents were stored overnight at 5°. The liquid phase was decanted and the solid was dissolved in 20% aqueous NaOH (16 mL). The solution was heated for 12 min to 90–95° and cooled before extraction with 4 × 10 mL of toluene. The toluene was dried over anhydrous $NaSO_4$ for 2.5 h and filtered. Dry HCl gas was bubbled through the toluene solution, which was stored at 5° overnight. The white microcrystalline product was collected by filtration and washed several times with Et_2O. Yield = 2.93 g (33%). Anal. Calcd for $C_5H_{14}NS_2Cl$: C, 31.99; H, 7.52; N, 7.46. Found: C, 33.91; H, 7.55; N, 7.70. IR (cm^{-1}) in KBr: 3005w, 2940m, 2680s, 2620s, 2560s, 2470s, 1475m, 1440m, 960w, 940w, 725w.

Bis(2-mercaptoethyl)(2-(methylthio)ethyl)amine (2). This ligand was synthesized according to a literature procedure[9] and was isolated by distillation at 110–125° and 0.025 mm.

Bis(2-mercaptoethyl)(2-(benzylthio)ethyl)amine Hydrochloride (3·HCl). This ligand was synthesized by a procedure analogous to that reported for **2**,[9] except that it was isolated as a hydrochoride salt. 2-(Benzylthio)ethylamine was prepared by reaction of aziridine and benzyl mercaptan. Aziridine was prepared by reaction of 2-aminoethylsulfate with NaOH according to a literature procedure.[47] A solution of aziridine (3.9 g, 0.10 mol) in MeOH (10 mL) was added slowly over a period of 20 min to a solution of benzyl mercaptan (12.4 g, 0.100 mol) (Aldrich) in MeOH (25 mL) with stirring. The reaction mixture was allowed to stand overnight. The solvent was then removed under vacuum and the residue was vacuum distilled at 120–130° and 3 mm. Yield = 12.1 g (74%).

2-(Benzylthio)ethylamine (1.17 g, 7.00 mmol) was added to a tube fitted with a Teflon high vacuum stopcock containing ethylene sulfide (1.05 g, 17.5 mmol) (Aldrich) dissolved in toluene (5 mL). The tube was then sealed, shaken, and allowed to stand at room temperature for 14 h. The tube was then immersed in an oil bath at 110° for 30 h. The solution was cooled to room temperature and filtered to remove a small amount of white solid. Dry HCl gas was passed into the solution, holding the temperature near 0° with an ice bath. An oil mixed with solid separated. The mixture was cooled for 5 h at −20°. The crude product (a viscous oil) was separated by removing the solvent via syringe and was then dissolved in warm EtOH (10 mL). Addition of Et_2O (15 mL) caused the solution to become cloudy. The mixture was allowed to stand at −20° overnight. The product, a gummy white solid, was collected and then dried under vacuum. Yield = 1.55 g (69%). The ligand was analyzed as its Ni complex (vide infra). IR (cm^{-1}) in KBr: 2980m, 2940m, 2630m, 2550s, 2500s, 1500m, 1460s, 1435s, 740s, 700s.

Bis(2-mercaptoethyl)(3,3-diphenylpropyl)amine Hydrochloride (4·HCl). 3,3-Diphenylpropylamine (3.00 g, 14.2 mmol) (Aldrich) was dissolved in toluene (10 mL) and added to a tube fitted with a Teflon high vacuum stopcock containing ethylene sulfide (2.13 g, 35.5 mmol) (Aldrich) dissolved in toluene (2.5 mL). The tube was then sealed, shaken, and allowed to stand at room temperature for 19 h. The tube was then immersed in an oil bath at 110° for 25 h. The mixture was cooled to room temperature and filtered to remove a small amount of white solid. Dry HCl gas was passed into the solution, holding the temperature near 0° with an ice bath. An oil formed and the mixture was allowed to stand at −20° overnight. The toluene was than removed via syringe and the crude product was dried under vacuum. The oil was then purified by first dissolving it in EtOH (10 mL), filtering the solution, and then adding Et_2O (25–30 mL). The resulting cloudy mixture was allowed to stand at 0° overnight and the product was then collected by filtration, washed with Et_2O, and dried under vacuum. Yield = 2.06 g (39%). A second crop was obtained upon addition of more Et_2O. Overall yield = 3.16 g (60%). Anal. Calcd for $C_{19}H_{26}NS_2Cl$: C, 62.01; H, 7.12; N, 3.81; S, 17.42. Found: C, 61.59; H, 7.23; N, 3.74; S, 17.10. IR (cm^{-1}) in KBr: 3100s, 3080s, 3050s, 2980s, 2900s, 1610m, 1505s, 1465s, 1045m, 765s, 720s.

Bis(2-mercaptoethyl)benzylamine Hydrochloride (5·HCl). Benzylamine (1.5 g, 14 mmol) (Aldrich) was added to a tube fitted with a Teflon high vacuum stopcock containing ethylene sulfide (2.0 g, 34 mmol) (Aldrich) dissolved in toluene (5 mL). The tube was then sealed, shaken, and allowed to stand at room temperature for 8 h. The tube was then immersed in an oil bath at 110° for 30 h. Upon cooling, the solution was filtered to remove a small amount of white solid. Dry HCl gas was passed into the solution, holding the temperature near 0° with an ice bath. The mixture was allowed to stand at −20° for 10 h before isolation of the crude product. The crude product, a white ppt, was purified by first dissolving it in EtOH (8 mL), filtering the solution, and then adding Et_2O (12 mL). Upon standing overnight, the solution deposited the white microcrystalline product, which was collected and dried under vacuum. Yield = 1.4 g (45%). Anal. Calcd for $C_{11}H_{18}NS_2Cl$: C, 50.08; H, 6.88; N, 5.31. Found: C, 50.67; H, 7.20; N, 5.07. IR (cm^{-1}) in KBr: 2980m, 2940m, 2930m, 2630m, 2550s, 2500s, 1500m, 1460s, 1435s, 740s, 700s, 510w.

Bis(2-mercaptoethyl) Sulfide (6). This ligand was purchased from Columbia Organic Chemical Company, Inc. and used without further purification.

$[Ni(1)]_2$. Anhydrous $Ni(OAc)_2$ (0.22 g, 1.2 mmol) was dissolved in warm MeOH (3 mL) and added dropwise to a stirred solution of **1·HCl** (0.22 g, 1.2 mmol) in warm MeOH (2 mL). Et_3N (0.16 mL, 1.2 mmol) was then added via syringe. The mixture was allowed to stand at room temperature for 24 h, whereupon microcrystalline product formed. The product was isolated via filtration, washed with ether and dried in vacuo. Yield = 0.29 g (62%). Anal. Calcd for $[Ni_2C_{10}H_{22}N_2S_4]$: C, 28.88; H, 5.33; N, 6.73. Found: C, 28.76; H, 5.17; N, 6.60. IR (cm^{-1}) in KBr: 2960m, 2920s, 2860m, 1550w, 1460s, 1315m, 1220m, 1200m, 1045m, 765s.

Samples labeled with ^{58}Ni used in FAB-mass spectroscopic investigations of isotopically labeled oxidation products were prepared from $^{58}Ni(OAc)_2 \cdot 4H_2O$ using the procedure outlined above. $^{58}Ni(OAc)_2 \cdot 4H_2O$ was prepared from ^{58}Ni metal (99.9%, U.S. Services Inc.) by first dissolving the metal in fuming HNO_3, evaporating the acid, and converting it to $Ni(OAc)_2 \cdot 4H_2O$ by repeated cycles of dissolution in hot acetic acid and evaporation.

$[Ni(2)]_2$. This complex was synthesized according to a published procedure.[10]

$[Ni(3)]_2$. Anhydrous $Ni(OAc)_2$ (0.85 g, 4.8 mmol) was dissolved in MeOH (5 mL) and added dropwise to stirred solution of **3·HCl** (1.55 g, 4.8 mmol) in MeOH (10 mL). Et_3N (0.48 g, 4.8 mmol) was then added via syringe. A black oil formed and was separated from the solvent via syringe and redissolved in DMF (15 mL). MeOH (15 mL) was added dropwise to the stirred DMF solution yielding the dark red-black crystalline product. The product was collected by filtration, washed with MeOH (3 x 5 mL) and dried under vacuum for 1.5 h. Yield = 0.90 g (54%). Anal. Calcd for $C_{26}H_{38}N_2S_6Ni_2$: C, 45.37; H, 5.56; N, 4.07. Found: C, 45.24; H, 5.60; N 4.03. A second crop was obtained by reducing the volume of the solution by 50% and storing it at −20° overnight. Total yield = 1.09 g (66%). IR (cm^{-1}) in KBr: 3020w, 2940m, 2860m, 1550m, 1465m, 1455m, 1220m, 1200m, 1080m, 1050m, 745m, 705s.

$[Ni(4)]_2$. Anhydrous $Ni(OAc)_2$ (0.14 g, 0.82 mmol) was dissolved in MeOH (3 mL) and added dropwise to a stirred solution of **4·HCl** (0.30 g, 0.82 mmol) in MeOH (3 mL). Et_3N (0.083 g, 0.82 mmol) was then added via syringe whereupon the dark red product precipitated from solution. After stirring for 30 min, the product was collected by filtration, washed with MeOH (3 mL) and with Et_2O and dried under vacuum. Yield = 0.18 g (56%). Anal. Calcd for $C_{38}H_{46}N_2S_4Ni_2$: C, 58.78; H, 5.97; N, 3.61. Found: C, 58.10; H, 6.17; N, 3.57. IR (cm^{-1}) in KBr: 3080w, 3060w, 3020s, 2930s, 2860m, 1600w, 1495s, 1450s, 1300w, 1190m, 1050s, 750s, 700s, 620m, 540m.

$[Ni(5)]_2$. Anhydrous $Ni(OAc)_2$ (0.51g, 2.9 mmol) was dissolved in MeOH (8 mL) and added dropwise to a stirred solution of **4·HCl** (0.76

---

(46) Cavallini, D.; Scandurra, R. *Biochim. Biophys. Res. Commun.* **1966**, *24*, 185.

(47) Reeves, W. A.; Drake, G. L., Jr.; Hoffanir, C. L. *J. Am. Chem. Soc.* **1951**, *73*, 3522.

g, 2.8 mmol) in MeOH (10 mL). Et_3N (0.29 g, 2.9 mmol) was then added via syringe whereupon the red product precipitated from solution. Yield = 0.62 g (77%). Anal. Calcd for $C_{22}H_{30}N_2S_4Ni_2$: C, 46.51 H, 5.32; N, 4.93. Found: C, 49.54 H, 6.85; N, 4.96. IR (cm^{-1})in KBr: 3020w, 2980m, 2920s, 2880m, 2850m, 1495m, 1450s, 1425m, 1030m, 720s, 700s.

[Ni(6)]$_2$. This complex was synthesized according to a published procedure.[11]

Et$_4$N[Ni(2)CN]. A solution of $Et_4N(CN)$ (0.058 g, 0.37 mmol) (Fluka) in DMF (2 mL) was added to a solution of [Ni(2)]$_2$ (0.10 g, 0.19 mmol) in DMF (5 mL) forming a dark green solution, which was stirred for 0.5 h. The solvent was removed under vacuum and the green solid was redissolved in CH_3CN (5 mL). Toluene (80 mL) was added, and the solution was stored at −20° for several days. During this time, dark green crystals of the product formed. These crystals were isolated by filtration, washed with Et_2O (2 × 5 mL) and dried under vacuum. Yield = 0.15 g (94%). Anal. Calcd for $C_{16}H_{35}N_3S_3Ni$: C, 45.29; H, 8.31; N, 9.90. Found: C, 45.29; H, 8.14; N, 9.72. IR (cm^{-1}) in Nujol: 2730w, 2100s (ν_{CN}), 1720w, 1590w, 1300m, 1270w, 1210w, 1185m, 1085m, 1040m, 980m, 920w, 900w, 860w, 800s, 750s, 725s.

These crystals were subsequently used for single crystal X-ray diffraction studies. The crystals are deliquescent and air sensitive, and were therefore handled only under an inert atmosphere in a glovebox.

Et$_4$N[Ni(6)CN]. A solution of $Et_4N(CN)$ (0.16 g, 1.0 mmol) in DMF was added to a solution of [Ni(**6**)]$_2$ (0.21 g, 0.50 mmol) in DMF (8 mL) forming a dark green solution, which was stirred for 4–6 h. Toluene (10 mL) was then layered on the DMF solution. Crystals were obtained by slow diffusion of the solvents in 8–10 days. These crystals were subsequently used in single-crystal X-ray diffraction studies. Yield = 0.24 g (65%). Anal. Calcd for $C_{13}H_{28}N_2S_3Ni$: C, 42.52; H, 7.68; N, 7.63. Found: C, 42.18; H, 7.84; N, 7.56. IR (cm^{-1}): 2980w, 2900w, 2840w, 2100s(ν_{CN}), 1485m, 1475w, 1440w, 1390m, 1365m, 1280w, 1260w, 1178s, 1100w, 1055w, 1000s, 870m, 845m, 790s, 660w.

Et$_4$N[Ni(1-O$_2$)CN]. This complex is conveniently obtained from the reaction of Et_4N[Ni(**1**)CN] in DMF solution, from which it precipitates. For example, reaction of [Ni(**1**)]$_2$ (47 mg, 0.11 mmol) and $Et_4N(CN)$ (39 mg, 0.25 mmol) with O_2 in DMF (2 mL) led to the formation of a yellow precipitate, which was collected by filtration in air, washed with Et_2O and dried under a stream of air. Yield = 38 mg (43%). Anal. Calcd for $C_{14}H_{31}N_3O_2S_2Ni$: C, 42.44; H, 7.89; N, 10.60. Found: C, 41.54; H, 7.68; N, 10.30. IR (cm^{-1}): 2950w, 2110 (ν_{CN}, m), 1483m, 1435w, 1390m, 1269w, 1170s (ν_aSO_2), 1045s (ν_sSO_2), 1023m 999w, 875w. Additional product may be obtained by adding toluene to the DMF filtrate (total yield = 73%).

Samples prepared using isotopically enriched O_2 for IR and FAB-mass spectroscopic studies were obtained in a similar manner using ^{58}Ni labeled [Ni(**1**)]$_2$ and $^{16}O_2$ (99.993%, U.S. Services, Inc.) and $^{18}O_2$ (99%, U.S. Services Inc.). An $^{16}O_2/^{18}O_2$ gas mixture was prepared to approximate proportions using manometry. The gas mixture obtained was determined to be 59% $^{16}O_2$ and 41% $^{18}O_2$ from the relative intensities of the dilabeled and unlabeled parent ion peaks in the mass spectra obtained from the oxidized complexes.

The exchange of sulfinato oxygen atoms with O_2 was examined by exposing a solution of Et_4N[Ni(**1-^{16}O$_2$**)CN] (32.6 mg) in DMF (5 mL) to $^{18}O_2$ for 8 h. The product was isolated by removing the solvent under vacuum, washing with Et_2O, and drying under vacuum. The product was analyzed by FAB mass spectroscopy.

Et$_4$N[Ni(2-O$_2$)CN]. This complex was prepared and crystallized as previously reported.[7] Samples prepared using isotopically enriched O_2 for IR and FAB-mass spectroscopic studies were obtained in a similar manner using $^{18}O_2$ (97–98%, Cambridge Isotope Laboratories) and natural abundance O_2. The gas mixture obtained was determined to be 54% $^{18}O_2$ and 46% $^{16}O_2$ based on the intensity of the dilabeled and unlabeled parent ion peaks in the mass spectra. The intensity of these peaks were corrected for contributions to the dilabeled mass originating from the presence of natural abundance Ni, and neglecting the contribution of ^{17}O (natural abundance = 0.038%).

Et$_4$N[Ni(L-O$_2$)CN] (L = 3–5). The products of the oxygenation reactions were precipitated from 0.4 mM DMF solutions by the addition of toluene, followed by washing with Et_2O and drying under vacuum. For L = **3**, IR (cm^{-1}): 3400(br), 2990w, 2160m (ν_{CN}), 1650m, 1450m, 1400m, 1260w, 1175s (ν_aSO_2), 1040s (ν_sSO_2), 1000w, 875m, 710w, 620w, 440w. For L = **4**, IR (cm^{-1}): 3400(br), 2110m (ν_{CN}), 1600m, 1175s (ν_aSO_2), 1040s (ν_sSO_2), 1000w, 870w, 710w. For L = **5** IR (cm^{-1}) in KBr: 3450w, 2990m, 2925m, 2860w, 2115s (ν_{CN}), 1675w, 1600w, 1490s, 1460s, 1400m, 1270w, 1180vs (ν_aSO_2), 1052vs (ν_sSO_2), 1005m, 895w, 785m, 730m, 710w, 680m, 640w, 565w, 545w, 520w, 500w, 470w, 440m.

Physical Measurements. Electronic absorption spectra were obtained by using an OLIS 4300 Cary-14 system. Infrared spectra for routine characterization were obtained as KBr pellets or Nujol mulls on a Perkin-Elmer 783 IR spectrophotometer and calibrated with polystyrene. Relative intensities of the bands in a spectrum are indicated (w = weak, m = medium, s = strong, vs = very strong, br = broad), and assignments are indicated when they can be made with confidence. IR spectra obtained on isotopically labeled samples of the oxidized products were obtained as KBr pellets on a Mattson Cygnus-100 FT-IR.

Negative ion fast atom bombardment (FAB) mass spectra on Et_4N[Ni(**1-O$_2$**)CN] samples in a glycerol matrix were obtained by the Midwest Center for Mass Spectrometry at the University of Nebraska, Lincoln by using a VG-ZAB-T spectrometer with a Cs ion gun. The accelerating voltage was 8 keV. FAB-mass spectra on Et_4N[Ni(**2-O$_2$**)CN] samples in an MNBA matrix were obtained by the University of Minnesota Mass Spectrometry Service Laboratory, Minneapolis by using a VG-7070E-HF spectrometer. Xe was used as the bombarding atom beam. The accelerating voltage was 5 keV.

Microanalyses were performed by the University of Massachusetts Microanalysis Laboratory.

Measurements of the rates of the oxidation reactions were made using 2.00 mM solutions of $[Ni(L)CN]^-$ by monitoring the appearance of a peak near 325 nm in the electronic absorption spectrum of the products. In general, the $[Ni(L)CN]^-$ complexes were generated in situ from the dimers, $[Ni(L)]_2$, via addition of $Et_4N(CN)$. The use of isolated samples of [Ni(**2**)CN]$^-$ and [Ni(**6**)CN]$^-$ did not affect the rates obtained. The reactions were conducted in a double-walled glass vessel, which was thermostatted by a circulating water bath to ±0.1°. Oxygen was bubbled through the thermostatted solutions via a needle inserted through a rubber septum closure on the apparatus. Aliquots were withdrawn from the reaction mixture via syringe, and their electronic absorption spectra were taken in 1 mm path length optical cells in a thermostatted cell holder in the spectrophotometer. The cell was held at the same temperature using the water circulated from the reaction vessel jacket.

Experiments were run under pseudo-first-order conditions in $[O_2]$. Reactions employing 1 atm of O_2 and temperatures of 30°, 40° and 50° were followed for at least three half-lives in order to determine the pseudo-first-order rate constants by iterative fits of the data. The order of the reaction with respect to $[O_2]$ was determined by varying the partial pressure of O_2 in an N_2/O_2 gas mix from 0.2–1.0 atmospheres using a Matheson model 7351H gas mixing apparatus, and employed rate constants from the first 100 min of the reaction. The enthalpy, ΔH^*, and entropy of activation, ΔS^*, were calculated using the Eyring relationship.[48]

Oxygen uptake measurements were made to determine the stoichiometry of the oxidation reactions. These measurements were made manometrically by using an apparatus similar to the one described by Chen and Martell.[22] The same reaction vessel used for the kinetic measurements was employed, and a circulating water bath was used to maintain the temperature at 30.0 ● 0.5°. In a typical measurement, 80–100 mg of $[Ni(L)]_2$ (0.2 mmol) and 1 equiv/Ni of $Et_4(CN)$ (Fluka) were placed in the reaction vessel, which was then evacuated. DMF (5 mL) was added through a septum and the apparatus was filled with O_2 following dissolution of the complex. The volume of oxygen absorbed by the complex was monitored over time until 3–4 successive readings were unchanged. The amount of oxygen absorbed (0.4 mmol, 10 mL) was corrected for the uptake of O_2 by DMF over the same period of time using measurements made on the pure solvent.

X-ray Structure Determinations. All X-ray crystallographic studies were done with an Enraf-Nonius CAD4 diffractometer and graphite monochromated molybdenum radiation. Details of the experimental procedures have been described previously.[49]

Crystals were mounted under N_2 in thin walled glass capillaries which were sealed. Data was collected using the θ–2θ scan mode.

The structures were solved by use of direct methods and difference Fourier techniques and were refined by full matrix least-squares.[50] All computations were performed on a MicroVAX II computer using the Enraf-Nonius SDP system of programs. Crystallographic data are summarized in Table II.

---

(48) Wilkins, R. G. *The Study of Kinetics and Mechanism of Reactions of Transitions Metal Complexes*; Allyn and Bacon, Inc.: Boston, MA, 1974; p 81.

(49) Sau, A. C.; Day, R. O.; Holmes, R. R. *Inorg. Chem.* **1981**, *20*, 3076.

(50) The function minimized was $\sum w(|F_o| - |F_c|)^2$, where $w^{1/2} = 2F_oL_p/\sigma_I$.

X-ray Study for $Et_4N[Ni(\mathbf{2})CN]$. Only crystals of poor quality (broad peaks, weak diffraction) could be obtained for the study. The lime green crystal that was selected for data collection was the point cut from a spearhead shaped mass and had maximum dimensions of 0.28 × 0.40 × 0.48 mm. A total of 2407 independent reflections ($+h,+k,\pm l$; $3° \leq 2\theta_{MoK\alpha} \leq 43°$) was measured. No corrections were made for absorption.

It was not possible to refine C6 and C7 of the dangling thioether group anisotropically and these two atoms were treated as isotropic scatterers. The remaining non-hydrogen atoms were refined anisotropically. Hydrogen atoms were included in ideal positions as fixed isotropic scatterers. The final refinement was based on 1678 reflections with $I \geq 3\sigma_I$. The maximum density in a final difference Fourier synthesis was in the immediate vicinity of the Ni atom.

X-ray Study for $Et_4N[Ni(\mathbf{2\text{-}O_2})CN]$. The orange crystal used for the study was cut from the end of a pointed lath and had approximate dimensions of 0.28 × 0.25 × 0.44 mm. A total of 3427 independent reflections ($+h,+k,\pm l$; $3° \leq 2\theta_{MoK\alpha} \leq 48°$) were measured. An empirical absorption correction based on ψ-scans was applied (relative transmission factors from 0.958 to 1.000 on I).

Non-hydrogen atoms were refined anisotropically. Hydrogen atoms were included in ideal positions as fixed isotropic scatterers. The final refinement was based on 2339 reflections with $I \geq 3\sigma_I$.

X-ray Study for $Et_4N[Ni(\mathbf{6})CN]$. The lath-like crystal used for the study had dimensions of 0.30 × 0.35 × 0.60 mm. A total of 1389 independent reflections was measured ($+h,+k,+l$; $3° \leq 2\theta_{MoK\alpha} \leq 45°$). An empirical absorption correction based on ψ-scans was applied (from 0.851 to 1.000 on I).

The structure is disordered with two clearly discernible positions for sulfur atom S3. It was not possible to resolve separate positions for other atoms in the anion. All non-hydrogen atoms were refined anisotropically. Hydrogen atoms of the cation were included as fixed isotropic scatterers in ideal positions. Hydrogen atoms of the disordered anion were omitted. The final refinement was based on 858 reflections with $I \geq 3\sigma_I$.

Acknowledgment. We acknowledge the Midwest Center for Mass Spectrometry, which is funded in part by NSF Grant DIR9017262, for providing some of the mass spectral data and NIH Grant GM-38829 (M.J.M.) for support of this research.

Supplementary Material Available: Figures showing mass spectra for $[Ni(\mathbf{2\text{-}O_2})CN]^-$ over the mass range of 100 or 200–500 mass units and tables of atomic coordinates, anisotropic thermal parameters, bond lengths and angles, and hydrogen atom parameters for $Et_4N[Ni(\mathbf{2})CN]$ (Tables S1–S4), $Et_4N[Ni(\mathbf{2\text{-}O_2})CN]$ (Tables S5–S8), and $Et_4N[Ni(\mathbf{6})CN]$ (Tables S9–S12) (22 pages). Ordering information is given on any current masthead page.